DESIGN AND OPTIMIZATION OF A COLD ENERGY AND WASTE HEAT UTILIZATION SYSTEM FOR LNG-POWERED SHIPS WITH POST-COMBUSTION CARBON CAPTURE

Shouguang YAO*, Jing SUN, Minjie XIA, Chao YING, Junwei YANG

School of Energy and Power, Jiangsu University of Science and Technology, Zhenjiang, Jiangsu 212003, China

*Corresponding Author; E-mail: zjyaosg@126.com

Abstract: *The introduction of dual-carbon targets has accelerated LNG fuel adoption on vessels and driven the advancement of carbon capture technologies. This study's aim is a 37000-deadweight tonnage liquified natural gas dual-fuel powered ship, for which chemical absorption carbon capture is applied, utilizing flue gas and liquified natural gas to supply the process's heat and cold energy. Then a system with efficient utilization of energy and carbon capture for the LNG dual-fuel ship is designed, coupling the waste heat onboard with transcritical CO_2 and organic Rankine cycle on the principle of energy cascade utilization. The system is simulated using Aspen HYSYS and the exergy analysis is carried out for this system. Then the working fluid is optimized for the system. After that, through the genetic algorithm, the system's operating parameters are further optimized. Additionally, the system's economic analysis is also performed. It is shown that the scheme's exergy efficiency reaches 39.98%, and the expected cost-recovery cycle is 4.75 years.*

Keywords: *LNG, waste heat recovery, carbon capture, exergy efficiency*

1. Introduction

Currently, 90% of international trade (in terms of commodity weight) is transported by ships. Approximately 3% of the world's carbon emissions come from the shipping industry, one of the carbon-intensive industries [1]. Currently, CO_2 emission reduction measures in the shipping industry mainly include use of clean fuels [2], recovery of waste heat [3], and carbon capture and storage technology [4].

As somewhat a cleaner energy source, natural gas is now widely employed for its high calorific value and light pollution characteristics [5]. In comparison to conventional fuel oil, ships can decrease CO_2 emissions by 20% and NO_x emissions by 90% using natural gas fuel, and produce almost no SO_x and PM. Liquified natural gas (LNG) in ship tanks is the form of natural gas that is preserved for storage and transportation, and has to be gasified in order to be fed to the main engine for burning. LNG discharges roughly 830 kJ/kg of cold energy during vaporization [6], and failure to efficiently make use of the cold energy will result in a huge waste of energy and cause harm to the marine environment.

Using LNG fuel alone will only slow down the growth of carbon emissions, but will not meet IMO's increasingly stringent greenhouse gas reduction requirements. It has been found that carbon capture, utilization and storage (CCUS) technologies hold great potential in CO_2 emission reduction.

Pre- [7], post- [8] and oxygen-rich combustion capture [9] are three main categories into which carbon capture technologies are classified. Both oxygen-rich combustion capture and pre-combustion capture require massive modifications to the existing engine structure and materials [8], which are costly. The post-combustion carbon capture (PCC) needs only simple improvements on the existing ship structures and equipment with a lower retrofit cost, and it is technically more mature than the other two carbon capture methods [10]. Therefore, in the short run, the post-combustion capture offers the best practical way of achieving carbon capture in shipping. Compared with adsorption and membrane separation, chemical absorption, as one type of PCC, is a technically mature and commercially widely used method. Besides, it has a higher absorption efficiency and is suitable for low CO_2 load conditions. However, solvent regeneration demands a large heat input. High heat demand makes chemical absorption difficult to implement on conventional ships.

The flue gas emitted from ships contains a large quantity of medium and low heat that can be recovered [11]. If the waste heat in the flue gas can be utilized to supply heat for the regeneration of the solvent for chemical absorption capture, it will make it possible to apply the chemical absorption to ships. Luo et al. applied solvent carbon capture to diesel ships for the first time, utilizing ship flue gas to provide heat for carbon capture. For the chemical absorption capture, an extra gas turbine was needed to supply heat and electricity. The entire energy efficiency was 42.16%, according to the results. And the carbon capture efficiency was 90% [12]. Feenstra et al. took a small inland waterway vessel and a cargo ship as research objects, and investigated the feasibility of carbon capture rate up to 90% or 60%, at 30% MEA and 30% PZ solvents respectively, using flue gas and LNG as heat and cold sources, separately [13]. Van Den Akker, for an 8000 DWT general cargo ship, used flue gas and LNG as heat and cold sources for carbon capture, and found that a 90% CO_2 capture rate could be achieved for the ship. Besides, feasibility study was did on the spatial placement of the carbon capture equipment and the storage of CO_2 on board [14]. The above references have studied the feasibility of using flue gas heat for carbon capture onboard. However, apart from the portion of heat needed for carbon capture, which is provided by the flue gas, residual waste heat onboard has not been efficiently utilized, which leads to the under-utilization of low and medium temperature waste heat on ships. In the context that people's pursuits of low carbon emission and efficient energy utilization have been becoming more and more intense, it is of significant value to build an efficient energy utilization system with carbon capture onboard, recovering both the cold energy in LNG and waste heat onboard.

In this study, for a 37000 t LNG-powered ship, a full power generation energy utilization system with carbon capture is designed. It utilizes waste heat at low- and medium-temperature onboard coupled with a Rankine cycle module with 2-stage cascade. Besides, to get the most out of the existing energy onboard, heat for solvent regeneration is obtained from the flue gas, and cold for carbon dioxide liquification is supplied by LNG. Carbon capture of flue gas is based on the solvent chemical absorption capture, which reduces the carbon emission onboard. The working fluid and operational parameters optimization improve the system's exergy efficiency, which brings considerable economic and environmental benefits.

2. System design

2.1. Main engine technical parameters

In this work, a 37000 t LNG dual-fuel powered ship taken as the target of the research, the vessel's main engine model is YMD-WARTSILA 5rt-flex50DF. For most of the marine engines run continuously at 75%-85% of the rated power, this study sets the target ship to run at 85% of the rated power. According to the marine engine manual given by Wärtsilä, Table 1 displays the main engine's parameters. In addition, the intake pressure of LNG does not exceed 1.6 MPa [15].

Table 1 The major parameters of the main engine

Parameter	Value
Host power (kW)	6120
Rational speed (rpm)	117.5
Engine exhaust temperature (℃)	281
Engine exhaust mass flow (kg/s)	14.5
Engine pilot oil consumption (kg/h)	10.4
LNG gas consumption of main engine (kg/h)	866.6
Main engine inlet temperature (℃)	0-45

2.2. System process design

The monoethanolamine solvent (MEA) has been widely used in the chemical absorption process on account of its good absorption effect and low cost [16, 17]. In this study, a MEA solution with a concentration of 25% is selected as the absorbent. Furthermore, because the flue gas and LNG, respectively, supply the heat and cold energy needed for the carbon capture process (without adding any external heat and cold), the quantity of heat that is available in the flue gas and the cold in the LNG determine the CO_2 capture rate. This study analyses the design of two modules: a chemical absorption carbon capture module and a Rankine cycle module with 2-stage cascade. The process is depicted in Fig. 1.

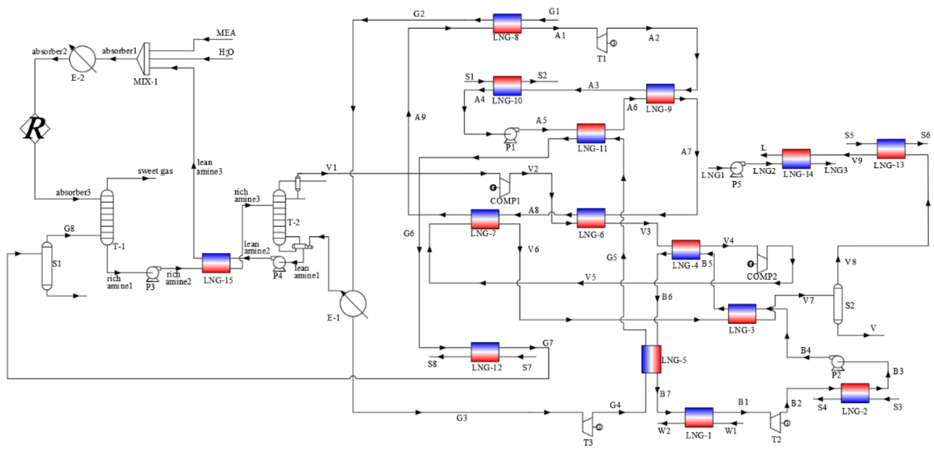

Fig. 1 A cold energy and waste heat utilization system for LNG-powered ships with post-combustion carbon capture

Following the turbocharger's emission of the flue gas, the transcritical CO_2 cycle is supplied heat by flue gas in the heat exchanger LNG-8. Afterwards the flue gas goes into the heat-exchanger E-1 to supply heat that solvent regeneration requires in the desorption tower. It flows through the exhaust gas turbine T3 to expand in order to make use of its residual heat and kinetic energy, and the flue gas gets into the heat exchanger LNG-5 to contribute heat that is necessary for the ORC. For the purpose of fully utilizing the flue gas's remaining heat, the flue gas heats the working fluid of T-CO_2 in LNG-11. And then it goes through heat exchanger LNG-12, being cooled to 40 ℃ by seawater.

Afterwards, the flue gas starts the process of CO_2 absorption. Firstly, it goes into the gas-liquid separator S1 to dewater, then, the flue gas and absorber into the absorption column from the bottom and top, respectively. The MEA solution and flue gas contact with counter-current, and fully react. So the carbon dioxide is removed and then top of the column releases the purified flue gas.

The rich amine is drained from the absorption tower bottom, then heated by lean amine in LNG-15. Then it enters the desorption tower, where the absorber regeneration is completed and carbon dioxide is desorbed out through the heat energy supplied by the flue gas. The tower top exhausts desorbed CO_2. After that, the top gas of the tower is compressed to 700 kPa by COMP1, and goes into heat exchanger LNG-6 to give heat for the T-CO_2 cycle. Then the CO_2-rich gas transfers heat to the working fluid (R600) of ORC (R600) in LNG-4, and is compressed to 16 bar by COMP2. After that, the CO_2-rich gas goes into heat exchanger LNG-7 to transfer heat to the working fluid of T-CO_2. Then it enters LNG-3 to be cooled down to 45 °C by the working fluid of ORC. It enters a gas-liquid separator S2 to remove water, and afterwards transfers heat to seawater in LNG-13, being lowered in temperature. Then it is liquefied by LNG in LNG-14 and the purity of liquid carbon dioxide reaches 99%. Between the critical point (73.8 bar, 31.1 ℃) and the three-phase point (5.18 bar, 156.6 ℃), carbon dioxide can be liquified at a variety of pressures. In this paper, using two stages of compression and intermediate cooling, carbon dioxide is pressurized to 16 bar, then liquified by LNG. The lean amine is excluded from the bottom of the tower, cooled down through the heat exchanger LNG-15, and then complemented with MEA and water. After that it is cooled down by seawater in E-2, and enters the absorption column to start the next carbon capture process of the flue gas.

After LNG is released from the storage containers, a pump pressurizes it to 1.4MPa. Later on, it is heated up to 15.8 °C by CO_2 stream in LNG-14. After that, NG is supplied to the main engine.

Pump P1 pressurizes the working fluid (CO_2) of T-CO_2 cycle. The flue gas preheats the working fluid in heat exchanger LNG-11. Then the working fluid is supplied with heat in the regenerator LNG-9. After successively flowing through heat exchanger LNG-6 and LNG-7 to be heated by the CO_2-rich stream, it goes into heat exchanger LNG-8 to be heated by flue gas. Going into the turbine T1 to expand, then it flows through the regenerator LNG-9 and the seawater cooler LNG-10. Afterwards, it is sent to the pump P1 to be pressurized, forming a complete T-CO_2 cycle.

The working fluid (R600) of ORC is pressurized by pump P2. It flows successively into the LNG-3 and LNG-4 to be heated by the CO_2-rich stream. It goes into heat exchanger LNG-5 to be heated by the flue gas and subsequently into heat exchanger LNG-1 to be further heated by cylinder liner water. Expanding through the turbine T2, then the working fluid goes into heat exchanger LNG-2 where it is cooled by seawater. Finally, it is pressurized by pump P2 to complete an organic Rankine cycle.

2.3. Physical parameters setting and assumptions

Table 2 displays the components of LNG. Besides, for a dual-fuel engine using diesel ignition, Table 3 gives the flue gas's composition. The following assumptions are made for purposes of modelling and simulating:

(1) Pumps efficiency is assumed to be 0.75; the adiabatic efficiency of compressors is assumed to be 0.75; turbines isentropic efficiency is assumed to be 0.8.

(2) Pressure drop of heat exchangers is set to 0.

(3) In the Rankine cycle module with two-stage cascade, the equation of state adopts the Peng-Robison formulation; in the carbon capture module, the acid gas-chemical solvent physical properties package is used for simulation.

(4) Seawater temperature is assumed to be 20 °C, and there should be no more than 5 ℃ temperature difference between its inlet and outlet, taking into account the environmental impact of seawater heat exchange.

(5) The environmental pressure is 101.3 kPa and the temperature is 25 °C.

Table 2 The components of LNG

Component species	Molar fraction (%)
Methane	95.8
Ethane	2.9
Propane	1.3

Table 3 The composition of the flue gas [23]

Component species	Molar fraction (%)
N_2	74
O_2	9.9
Ar	0.9
CO_2	4.8
H_2O	10.4

3. Simulation results and exergy analysis

The system is simulated by Aspen HYSYS to obtain simulation results at steady state conditions. It is shown that the system's overall exergy efficiency is 37.26% and the Rankine cycle module's exergy efficiency is 57.44%. Therefore, the efficiency of waste heat utilization in the Rankine cycle module is better than that in the total system. Exergy losses for heat exchangers in the Rankine cycle module are shown in table 4. The carbon capture module's key parameters are listed in Table 5.

Without any additional external heat or cold, for the quantity of the heat energy of the flue gas onboard and the cold energy released during LNG vaporization, the system's carbon capture rate that can be reached is 53%. The heat demand of the reboiler is 3.56 MJ/kg. Furthermore, the mass flow rate of CO_2 captured is 2063 kg/h, and its purity is 99%, which means that the system significantly reduces carbon emissions onboard.

As can be seen from Table 4, among all heat exchangers, LNG-12 and LNG-14 cause the largest losses. Because seawater cools the flue gas directly and CO_2 is cooled and liquified by the LNG, respectively. But, considering that LNG is a limited source of cold onboard, the cold energy released during LNG vaporization (-162 ℃ to 15.8 °C) at the main engine vaporization rate of the ship would only lower the temperature of carbon dioxide stream from 25 °C to -29 °C for mass flow rate of 2063 kg/h. So there's no way to avoid these two parts of exergy damage. Besides, LNG-8 has a great exergy loss that is secondary only to LNG-12 and LNG-14. But it is not possible to reduce this loss through the optimization of working fluid, because the cold fluid is the working fluid (CO_2) of T-CO_2. Furthermore, it can be observed that the LNG-2 shows the fourth largest exergy loss. As can be seen from the temperature-heat flow diagram of the cold and hot fluid in Fig. 2, the heat transfer curves for organic working fluid (R600) and seawater do not fit. Consequently, the large temperature differences of heat exchange result in the large exergy loss. Consequently, matching of the heat transfer curves can be optimized by the optimization of the working fluid (R600).

Table 4 Exergy losses of heat exchangers in the RC module

Equipment	Exergy income	Exergy payment	Exergy destruction	Exergy efficiency
LNG-1	53.94	56.40	2.46	0.96
LNG-2	8.46	24.95	16.49	0.34
LNG-3	2.30	3.95	16.49	0.58
LNG-4	1.69	5.76	4.07	0.29
LNG-5	104.5	120.18	15.68	0.8
LNG-6	3.27	3.90	0.63	0.84
LNG-7	3.28	3.95	0.66	0.83
LNG-8	72.80	103.27	30.47	0.7
LNG-9	33.37	26.32	7.05	0.79
LNG-10	9.10	2.80	6.3	0.31
LNG-11	12.53	15.19	2.66	0.82
LNG-12	72.71	9.34	63.36	0.13
LNG-13	0.46	0.12	0.34	0.26
LNG-14	38.79	157.02	118.23	0.25

Table 5 The main parameters of the carbon capture module

Rich loading	0.44
Lean loading	0.32
Rich amine3 temperature (℃)	104.6
Absorber3 temperature (℃)	30
Reboiler heat duty (MJ/kg CO_2)	3.56
Number of plates in the absorption tower	20
Number of plates in the desorption tower	20

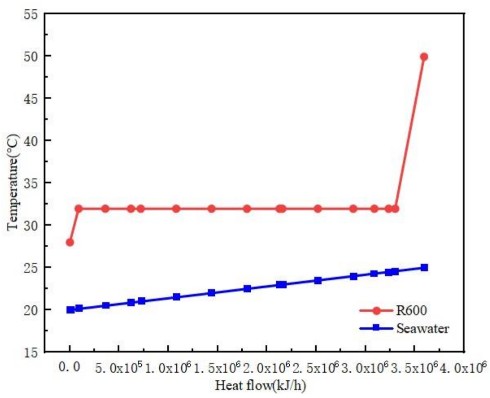

Fig. 2 Temperature-heat flow diagram of the cold and hot fluid

4. System optimization

4.1. Working fluid optimization

In accordance with the previous simulation and exergy analysis, the single working fluid (R600) in the ORC can be replaced with a non-azeotropic mixture to further increase exergy efficiency. Mixed working fluids show better matching with hot and cold sources due to temperature slip during isobaric condensation and evaporation [18].

To choose appropriate mixed working fluid, the temperature-entropy curves of typical pure working fluids (ethane, propane, R1270) are compared with the temperature-entropy curve of seawater, which is depicted in Fig.3. It is evident that propane and R1270 fit better with the seawater's temperature-entropy curve in the temperature band 20-30 °C. Therefore, in the organic Rankine cycle, propane and R1270 are selected to be mixed with R600, and Fig. 4 illustrates the system's exergy efficiency and output power after mixing the working fluids according to different ratios.

It can be seen that when the R600: propane: R1270 ratio is 45:1:4, the system's exergy efficiency and output power are at their maximum. Fig. 5 shows the heat transfer curves in heat exchanger LNG-2 after the working fluid optimization, and it is concluded that, after optimization of the working fluid, there is a closer match between the heat transfer curves of the mixed working fluid and seawater. Besides, after the working fluid optimization, the system's overall exergy efficiency is 37.35%, which is 0.09% higher, and the output power is 438.5 kW, which is 1.8 kW higher than before optimization of the working fluid. The Rankine cycle module's exergy efficiency reaches 57.52%.

While LNG-2 isn't a major contributor to the system exergy losses, the improvements after optimization of the working fluid are not obvious. So as to further optimize this system, some sensitive parameters ought to be selected and optimized.

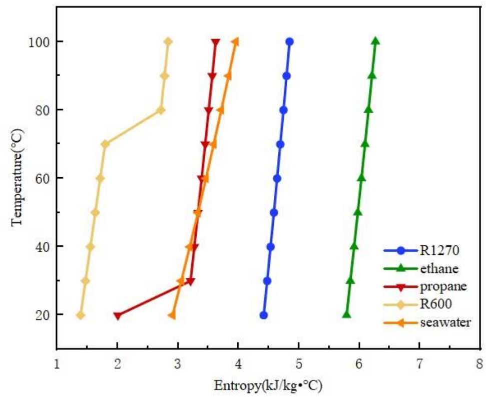

Fig. 3 Temperature-entropy diagram of typical pure working fluids(300kPa) and LNG (1400kPa)

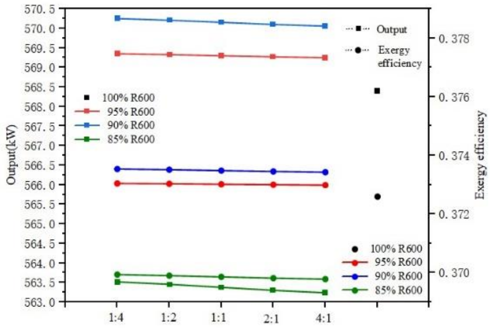

Fig. 4 Variation of total exergy efficiency and output of the system with different mixing ratios of propane and R1270

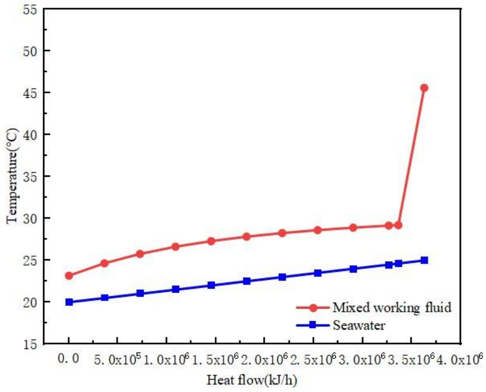

Fig. 5 The heat transfer curves in heat exchanger LNG-2 after the working fluid optimization

4.2. Sensitive parameters optimization

By genetic inheritance and repeated iterations of the original population, the genetic algorithm, a potent optimization technique, achieves survival of the best by handling numerous members in a population at once. In addition, the genetic algorithm doesn't need the objective function to be continuous, while it can find more original points to solve for. Therefore, the technique has good capability of global optimization.

Using the objective function as the evaluation index, different objective functions bring different optimization results. Taking the system's exergy efficiency as the target function, Fig. 6 illustrates how the selected sensitive parameters affect the system's overall exergy efficiency. The slope of curves represents the sensitivity of associated parameters.

According to Fig. 6, it is evident that the evaporation pressure and condensation pressure of T-CO_2 and ORC can greatly affect the system's overall exergy efficiency. Consequently, these four parameters are selected as sensitive for system optimization. So as to assure the normal operation of each piece of equipment, each sensitive parameter's value range is determined and indicated in table 6. The MATLAB genetic algorithm is invoked to optimize sensitive operational parameters with the system's exergy efficiency being regarded as the target function.

Through the use of the genetic algorithm for global parameters optimization, the system's overall exergy efficiency is improved. Table 7 indicates that the overall efficiency of the system is increased from 37.35% to 39.98% and after parameters optimization, the net output power is 485.3

kW, which is an increase of 46.8 kW. Furthermore, the Rankine cycle module's exergy efficiency reaches 58.88%.

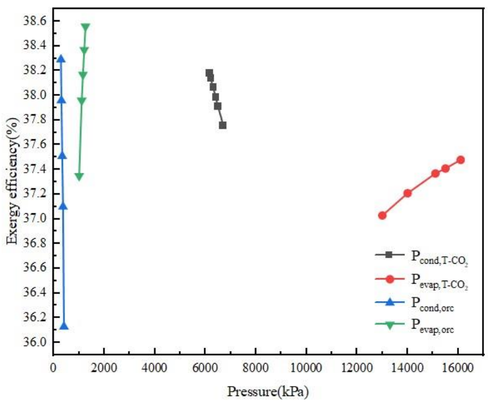

Fig. 6 Effect of some parameters on the system's exergy efficiency

Table 6 Range of values of sensitive parameters and optimized values

Parameter	Lower limit(kPa)	Upper limit(kPa)	Optimized value(kPa)
$P_{con,T-CO_2}$	6150	8000	6230
$P_{evap,T-CO_2}$	10000	16100	15640
$P_{con,ORC}$	280	500	280
$P_{evap,ORC}$	1000	1250	1203

Table 7 Comparison of system performance before and after optimization of sensitive parameters

<table>
<tr><th rowspan="2">Module</th><th colspan="2">Before optimization</th><th colspan="2">After optimization</th></tr>
<tr><th>Net output power(kW)</th><th>Exergy efficiency (%)</th><th>Net output power(kW)</th><th>Exergy efficiency (%)</th></tr>
<tr><td>Rankine cycle</td><td rowspan="2">438.5</td><td>57.52</td><td rowspan="2">485.3</td><td>58.88</td></tr>
<tr><td>System</td><td>37.35</td><td>39.98</td></tr>
</table>

5. Economic analysis

The feasibility of a system application cannot be completely assessed using thermodynamic analysis alone. So further consideration of economic factors needs to be taken into account. Table 8 displays the functions of initial investment cost of primary components. Table 9 presents the expected cost of initial investment for each piece of equipment in the optimized scheme.

Table 8 The functions of initial investment cost

Component	Investment cost function	Ref
Turbine	$Z_{turb} = \frac{479.34 \bullet \dot{m}}{0.92 - \eta_{is,turb}} \bullet ln(\frac{P_{in}}{P_{out}})[1 + \exp(0.036 \bullet T_{in} - 54.4)]$	[19, 20]
Pump	$Z_{pump} = 800 \bullet (\frac{\dot{W}_{pump}}{10}) \bullet (\frac{1 - \eta_{pump}}{\eta_{pump}})^{0.5}$	[19]

Heat exchanger	$Z_{HX} = 130 \bullet (\frac{A_{HX}}{0.093})^{0.78}$	[19, 20]
Gas compressor	$Z_{Gas,comp} = \frac{35 \bullet \dot{m}}{0.9 - \eta_{is}} \bullet r_p \bullet \ln(r_p)$	[19]
Absorber and Stripper	$Z_p = F_{BM1} \cdot Z_{towers} + F_{BM2} \cdot Z_{trays}$ $log_{10}Z_{towers} = k_1 + k_2 log_{10}A + k_3[log_{10}A]^2$ $log_{10}Z_{trays} = k_1 + k_2 log_{10}A + k_3[log_{10}A]^2$ Towers: $k_1 = 3.4974; k_2 = 0.4485; k_3 = 0.1074$ Trays: $k_1 = 2.9949; k_2 = 0.4465; k_3 = 0.3961$ $F_{BM1} = 4.07;\ F_{BM2} = 1$	[21]

Table 9 Initial investment cost for each piece of equipment

Component	Initial investment cost (US $)
Turbine	7580.33
Pump	1669.7
Heat exchanger	407303.69
Compressor	620.61
Absorber and Stripper	1187047
Total	2627514.23

The operation and maintenance cost rate $Z_{OM,k}$ and the initial investment cost rate $Z_{CI,k}$ amount to the system's total investment cost rate [22]:

$$C_{total} = \sum_k (Z_{CI} + Z_{OM})_k \#(1)$$

$$Z_{CI,k} + Z_{OM,k} = \frac{Z_k \cdot \emptyset}{N \cdot 3600} \cdot CRF\#(2)$$

where, Z_k represents the initial investment, $\emptyset$ stands for the system's maintenance factor, set at 1.06 [26]; N stands for the system's annual operating hours, set at 7500 h [23]; The capital factor, denoted as *CRF*, is expressed as below [22]:

$$CRF = \frac{i(1+i)^{\tau}}{(1+i)^{\tau} - 1}\#(3)$$

where τ represents the system's life cycle, set at 15 years [24], i represents the annual interest rate, set at 0.12 [23].

EPC means the system's electricity production cost, which is described as [22]:

$$EPC = \frac{3600 \cdot C_{total}}{W_{net}}\#(4)$$

ANGR stands for the system's annual net generation revenue, which is expressed as [22]:

$$ANGR = 7500 \cdot (EP - EPC) \cdot W_{net}\#(5)$$

where EP stands for the electricity price for present ships, set at US$0.2/kWh [25].

Since the liquid CO_2 captured in the system can be sold as an extra product, ANTI means the system's annual total net income, which is defined by:

$$ANTI = ANGR + 7500 \cdot m_{CO_2} \cdot LCP\#(6)$$

where LCP represents the current price of liquid CO_2, set at US$17.3/t, and m_{CO_2} stands for the mass flow rate of the captured CO_2.

Thus, the system's payback period, denoted as *PBP*, which is expressed as:

$$PBP = \frac{Z_{k,total} \cdot \emptyset}{ANTI} \#(7)$$

On basis of the above equations, the system's revenue from annual net power generation after optimization is $320298. With the liquid CO_2 added to the overall value, the total annual net revenue is $588028. The system's initial investment cost is $2627514; the system's maintenance cost is $157651. Based on the above economic analysis, the system proposed in this study is projected to recover the investment cost in 4.75 years for the dual-fuel 37,000 t LNG ship.

6. Conclusion

In this study, a 37000 t LNG dual-fuel ship is studied as the target vessel. Using the chemical absorption carbon capture, this study designs the energy utilization system with carbon capture. This system is simulated using Aspen HYSYS and exergy analysis is completed. After the working fluid optimization and operational parameters optimization, this system's exergy efficiency is improved. In addition, the system after optimization is analyzed economically. The conclusions are as follows:

(1) Without any external cold and heat, the system achieves a CO_2 capture efficiency of 53%. Besides, the captured CO_2 has a 2063 kg/h mass flow rate and 99% purity.

(2) The low- and medium-temperature waste heat onboard is utilized as a heat source for a Rankine cycle module with two-stage cascade in addition to the portion of heat supplied by the flue gas for carbon capture module. As a result, this system's exergy efficiency attains 37.26%.

(3) The optimized ratio of the mixed working fluid in ORC is 45:1:4 for R600: propane: R1150.

(4) The system's efficiency is improved to 39.98% and the system's net output power is 485.3 kW after the operational parameters optimization. Besides, annual net revenue and costs of the optimized system are $588028 and $2627514 respectively. As a result, it is expected that the system's investment costs may be recovered in 4.75 years.

Reference

[1] Paul B, Iain S, Garcia K I, et al. How can LNG-fuelled ships meet decarbonisation targets? An environmental and economic analysis. Energy.2021; **227**.

[2] Wu S, Salmon N, Li M M-J, et al. Energy Decarbonization via Green H2 or NH3? ACS Energy Letters.2022; **7**(3): 1021-1033.

[3] Lion S, Vlaskos I,Taccani R. A review of emissions reduction technologies for low and medium speed marine Diesel engines and their potential for waste heat recovery. Energy Conversion and Management.2020; **207**.

[4] Huangying W, Junying Y, Wanjie S, et al. Ion exchange membrane related processes towards carbon capture, utilization and storage: Current trends and perspectives. Separation and Purification Technology.2022; **296**.

[5] Fahmy M F M,Nabih H I. Impact of ambient air temperature and heat load variation on the performance of air-cooled heat exchangers in propane cycles in LNG plants – Analytical approach. Energy Conversion and Management.2016; **121**.

[6] He T, Chong Z R, Zheng J, et al. LNG cold energy utilization: Prospects and challenges. Energy.2019; **170**.

[7] Chen X, Shi P, Yan S, et al. Application of CO2 capture technology before burning in IGCC power generation system. Journal of Chemical Industry and Engineering.2014(8): 3193-3201.

[8] Wang D, *Full Chain Analysis, Integration and Optimization of CO2 Capture, Utilization and Storage Technology.[D]*. 2020, Institute of Engineering Thermophysics, Chinese Academy of Sciences Beijing.

[9] Shouguang Y, Chen L,Yue W. Design and optimization of a zero carbon emission system integrated with the utilization of marine engine waste heat and LNG cold energy for LNG-powered ships. Applied Thermal Engineering.2023; **231**.

[10] Weisan H, Yishun S, Xuelai Z, et al. Research progress of carbon capture and storage (CCS) technology based on the shipping industry. Ocean Engineering.2023; **281**.

[11] Sanchez Fernandez E, *Novel process designs to improve the efficiency of postcombustion carbon dioxide capture*. 2013, TU Delft, Delft University of Technology.

[12] Luo X,Wang M. Study of solvent-based carbon capture for cargo ships through process modelling and simulation. Applied Energy.2017; **195**.

[13] Feenstra M, Monteiro J, Akker J T v d, et al. Ship-based carbon capture onboard of diesel or LNG-fuelled ships. International Journal of Greenhouse Gas Control.2019; **85**.

[14] Akker J, *Carbon capture onboard LNG-fueled vessels, a feasibility study*. 2017, MSc. Thesis, Marine Technology, Delft University of Technology, The Netherlands.

[15] Yao S, Shen X,Luo J. Design and optimization of LNG cold energy utilization scheme for dual fuel main engine of 37000DWT asphalt ship. International Journal of Green Energy.2021; **18**(12): 1289-1301.

[16] Ramezani R, Mazinani S,Di Felice R. A comprehensive kinetic and thermodynamic study of CO2 absorption in blends of monoethanolamine and potassium lysinate: experimental and modeling. Chemical Engineering Science.2019; **206**: 187-202.

[17] Fu K, Chen G, Liang Z, et al. Analysis of mass transfer performance of monoethanolamine-based CO2 absorption in a packed column using artificial neural networks. Industrial & Engineering Chemistry Research.2014; **53**(11): 4413-4423.

[18] He T, Ma H, Ma J, et al. Effects of cooling and heating sources properties and working fluid selection on cryogenic organic Rankine cycle for LNG cold energy utilization. Energy Conversion and Management.2021; **247**: 114706.

[19] Liu Y, Han J,You H. Exergoeconomic analysis and multi-objective optimization of a CCHP system based on LNG cold energy utilization and flue gas waste heat recovery with CO2 capture. Energy.2020; **190**: 116201.

[20] Zhang X, Liu X, Sun X, et al. Thermodynamic and economic assessment of a novel CCHP integrated system taking biomass, natural gas and geothermal energy as co-feeds. Energy Conversion and Management.2018; **172**: 105-118.

[21] Julio A A V, Castro-Amoedo R, Maréchal F, et al. Exergy and economic analysis of the trade-off for design of post-combustion CO2 capture plant by chemical absorption with MEA. Energy.2023; **280**.

[22] Bao J, Lin Y, Zhang R, et al. Effects of stage number of condensing process on the power generation systems for LNG cold energy recovery. Applied Thermal Engineering.2017; **126**: 566-582.

[23] Mosaffa A,Farshi L G. Exergoeconomic and environmental analyses of an air conditioning system using thermal energy storage. Applied Energy.2016; **162**: 515-526.

[24] Su Z, Ouyang T, Chen J, et al. Green and efficient configuration of integrated waste heat and cold energy recovery for marine natural gas/diesel dual-fuel engine. Energy Conversion and Management.2020; **209**.

[25] Zhang C, Liu C, Wang S, et al. Thermo-economic comparison of subcritical organic Rankine cycle based on different heat exchanger configurations. Energy.2017; **123**.

Submitted: 09.01.2024
Revised: 03.03.2024
Accepted: 12.03.2024